Dual Cylinder Drag Reduction Using PisoFOAM

Brianna Hillman[1], mrwood3[2], and scorteshernandez[2]

[1]University of Alabama
[2]Affiliation not available

December 14, 2018

Introduction

The study of fluid flow around cylinders is not a new topic of interest. It has come to be one of the classical problems of fluid mechanics. Cylinder-like architecture can be found in an array of things such as heat exchangers, cooling systems, cables, buildings and anything regarding air-flow and/or water-flow. Numerous studies have been done where the disturbance of cylinders in a close range can cause "significant changes in parameters of the aerodynamic characteristics, such as fluctuating lift and drag forces, time-averaged and fluctuating pressure distributions, Strouhal number, and vortex shedding patterns, when the spacing between the cylinders is changed," and all at a broad spectrum of Reynolds' numbers[1]. However, there are very few instances in which two cylinders will be perfectly aligned and our literature review findings reflect that. Nevertheless, many interesting discoveries uncovered in our search.

For instance, a study done by Carmo investigates the two- and three-dimensional numerical solutions of flow around pairs of cylinders. His findings state that for Reynolds numbers greater than 190, two-dimensional simulations are not sufficient enough to predict the Reynolds number to centre-to-centre pair of drag inversion [2]. In a somewhat similar fashion, another study investigates the fluctuating forces acting on two square prisms in a turbulent boundary layer in numerous arrangements. Sakamoto's findings declare that phase relationships exist between the fluctuating lift of the two prisms and the phase shift is proportional to the distance between the prisms [3].Although our simulations only investigate an arrangement of two cylinders, a study done by Price had an interesting find. His study investigated the fluid forces acting on a single cylinder in groups of two and three cylinders. His findings affirm that "the effect of cylinder displacement on the fluid forces of one cylinder in a group of three is very similar to that obtained with one cylinder in a group of two" [4]. One study even focused on the analysis others had performed in the past 10-20 years on finite flow around two "infinite" cylinders. Surprisingly, in Sumner's comprehensive review of the literature of flow around two circular cylinders of with the same diameter, his findings state that a "deeper insight into the flow physics will arise from more accurate numerical simulations at higher Reynolds number; however there is a general lack of experimental data at low Reynolds number to assist with the validation of current numerical simulations" [5].

Investigating the fluid flow around cylinders can provide a better understanding of the fluid forces in instances where more complex arrangements are involved. In our report, we investigate a way to reduce the fluid forces acting on two circular cylinders in a tandem arrangement exposed to an incompressible, turbulent fluid flow by changing the distance between the cylinders.

Problem Specification

The purpose of doing our analyses, as stated previously, was to minimize the collective drag forces over two tandem cylinders. The process towards getting this information involved, first and foremost, the creation of a baseline domain containing the two cylinders using a geometry text file. The distances between those cylinders were then altered, saved in new files, and meshed using Gmsh prior to being simulated upon. We increased the number of cells to refine the mesh and in return increase the accuracy of our results. The description of the overall domain created and the process of varying the distance between cylinders is described in the Domain Description section of the report. OpenFOAM's pisoFoam solver was used to run the simulations due to the assumptions that the fluid flowing around the cylinders was incompressible and that the effects of turbulence were large enough to be consequentially impact solver calculations. Information regarding the general equations involved with this solver, in addition to, specific ones for our simulations

are in the proceeding section of this report. The solver was ran twenty-two times, each time with a new iteration of distance between the cylinders. For all simulations, additional code was added which calculated the individual forces on each cylinder and then summed them to get the net forces on both cylinders. The relevant forces resulting from those simulations are shown in the Results section of the report. Based on these results, a conclusion was drawn for what the best distance to separate the cylinders was in order to minimize the collective drag over both.

Mathematical Modeling

As stated previously, the pisoFoam solver is an OpenFOAM solver which computes data from analyses relating to incompressible fluid flow. The piso- in pisoFOAM stands for Pressure Implicit with Splitting of Operators. The two main equations governing the pisoFoam solver are the Navier-Stokes Momentum Conservation Equation and the Continuity Equation. These two equations are shown below, respectively[6].

$$\frac{\partial u_i}{\partial t} + \frac{\partial u_i u_j}{\partial x_j} = -\frac{\partial P}{\partial x_i} + \nu \frac{\partial^2 u_i}{\partial x_j \partial x_j} + f_i \tag{1}$$

$$\frac{\partial}{\partial t} + \nabla \cdot u = 0 \tag{2}$$

The Navier-Stokes equation deals with the flow of incompressible fluid while the Continuity Equation is an equation relating to the Law of Conservation of Mass. This law states that mass cannot be created or destroyed within a system and energy transfers. However, for an incompressible fluid the density is constant. Thus the continuity equation reduces to the volume continuity equation shown below.

$$\nabla \cdot u = 0 \tag{3}$$

In the midterm, this solver was used to analyze laminar incompressible fluid flow. For this project, additional equations were necessary to perform analysis of turbulent, incompressible fluid flow. The RAS, or Reynold's Averaged Simulation model was used for our simulations. Upon choosing the RAS model, we then chose the $k-\epsilon$ model to apply to our simulation. The $k-\epsilon$ model is a two equation model. The two additional equations represent the turbulence kinetic energy k and the turbulence dissipation rate ϵ. These OpenFOAM version of the $k-\epsilon$ model equations for each of these is shown below, respectively[7].

$$\frac{D}{Dt}(\rho k) = \nabla \cdot (\rho D_k \nabla k) + G_k - \frac{2}{3}\rho(\nabla \cdot u)k - \rho\epsilon + S_k \tag{4}$$

$$\frac{D}{Dt}(\rho \epsilon) = \nabla \cdot (\rho D_\epsilon \nabla \epsilon) + \frac{C_1 G_k \epsilon}{k} - (\frac{2}{3}C_1 - C_{3,RDT})\rho(\nabla \cdot u)\epsilon - C_2 \rho \frac{\epsilon^2}{k} + S_\epsilon \tag{5}$$

The turbulence viscosity is acquired by:

$$\nu_t = C_\mu \frac{k^2}{\epsilon} \tag{6}$$

Table 1: Model Coefficients

C_μ	C_1	C_2	$C_{3,RDT}$	σ_k	σ_ϵ
0.09	1.44	1.92	0	1	1.3

Note that the third term on the right hand side of the turbulence dissipation rate equation incorporates the Rapid Distortion Theory contribution. Neither this nor buoyancy contributions were included in our analyses. The default $k-\epsilon$ model coefficients are stated in the table below and were used in our analyses.

The turbulence kinetic energy and turbulence dissipation rate were initialized using the equations shown below:

$$k = \frac{3}{2}(I|u_{ref}|)^2 \tag{7}$$

$$\epsilon = \frac{C_\mu^{0.75} k^{1.5}}{L} \tag{8}$$

where *I* is the turbulent intensity, u_{ref} is the reference, or initial, velocity and *L* is the characteristic length. Turbulent intensity is a dimensionless quantity and is measured on a scale of 0-20, with [0,1] meaning the turbulence present is of low intensity, [1,5] is medium intensity and [5,20] is high intensity. Turbulent intensity is calculate based on the Reynold's number, as shown.

$$I = 0.16 Re^{-\frac{1}{8}} \tag{9}$$

One of the interesting properties about the $k-\epsilon$ turbulence model is that it requires near wall treatment. Because of this, the boundaries, or patches, of the elements in our domain had to be set to wall functions. For instance, in the *0* directory where the initial value files of our simulations are contained, instead of the surfaces having a "type" of *fixedValue* or *zeroGradient*, they had "types" such as *kqrWallFunction* or *epsilonWallFunction* depending on their respective folders.

Domain Description

The tandem cylinders for which the drag was being reduced were inset in a larger rectangular domain. The aforementioned domain had a length span of five meters and a width of a single meter. Both modeled cylinders had a diameter of a tenth of a meter. One cylinder's location was kept constant, resting at one meter from the leftmost side of the length span and centered on the half-width of the width span, for all simulations. The second cylinder was moved along the length span with respect to the position of the first cylinder by multiplying the first cylinder's location along the length of the domain by an arbitrary coefficient, A. The distance along the width span of the second cylinder was kept constant with respect to the first. The domain display for when coefficient A was set to two, meaning that the second cylinder was two meters from the leftmost edge of the domain, is modeled below in Figure 1.

Every time a new simulation was undertaken, the coefficient A and the distance between the cylinders was recorded. All coefficients of A which were used to model the cylinders as well as the corresponding

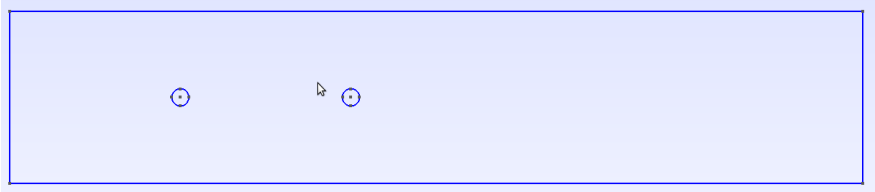

Figure 1: Model of the Domain when A = 2

Table 2: Coefficients for A and Corresponding Distances

A	0.6	0.75	0.8	0.85	0.9	1.1	1.15	1.175	1.2	1.25	1.3
Distances (m)	0.3	0.15	0.1	0.05	0	0	0.05	0.075	0.1	0.15	0.2
height A	1.35	1.5	2	2.25	2.5	2.75	3	3.25	3.5	3.75	4
Distances (m)	0.25	0.4	0.9	1.15	1.4	1.65	1.9	2.15	2.4	2.65	2.9

distances between the nearest most points of the two cylinders post modeling were recorded. These values are shown below in Table 2.

For simulations corresponding to A equals 0.6 through A equals 0.9, the second cylinder was modeled to the left of the stationary cylinder. Thus, the distances for those A values are between the moving cylinder's rightmost point and the leftmost point of the stationary cylinder. For simulations corresponding to A equals 1.1 through A equals 4, the second cylinder was modeled to the right of the stationary cylinder. Therefore, for these simulations the distance is between the rightmost point of the stationary cylinder and the leftmost point of the moving cylinder. For simulations at A equals 0.9 and A equals 1.1, the cylinders were adjacent which was why their distances are shown to be 0 meters in the table.

Patches and Parameters

When implementing the meshed geometries with pisoFoam, areas of the domain had to be defined. The "outlet" for the simulations corresponded to the area facing diagonally to the right in Figure 2 below. The "inlet" was symmetic to the "outlet" at the other end and both the "inlet" and "outlet" were physical patches. This meant that these were the patches for which parameters were added. The area in Figure 2 facing diagonally to the left was defined as "bottom".

The area defined as "top" was symmetric to the "bottom" on the other side of the model. The "circles" are simply the circles used to model the cylinders. All three of these entities were set as walls as needed for the k-epsilon model as mentioned previously. The remaining patches parallel with the circles made during the creation of the cylinders were the denoted as "front" and "back" empty patches meaning that they were assumed to have data that was inconsequential to the overall calculations and thus, only would be calculated in 2-dimensions to save time.

Paramterers were provided to pisoFoam files in order to run the general simulation. For the inlet, an input velocity, V, and an input pressure had to be specified. A flow velocity of eight meters per second and zero-gradient pressure was chosen for our simulations. At the outlet, the pressure was set to zero pascals.The Reynolds Number was calculated using the input velocity within the Reynolds Number formula

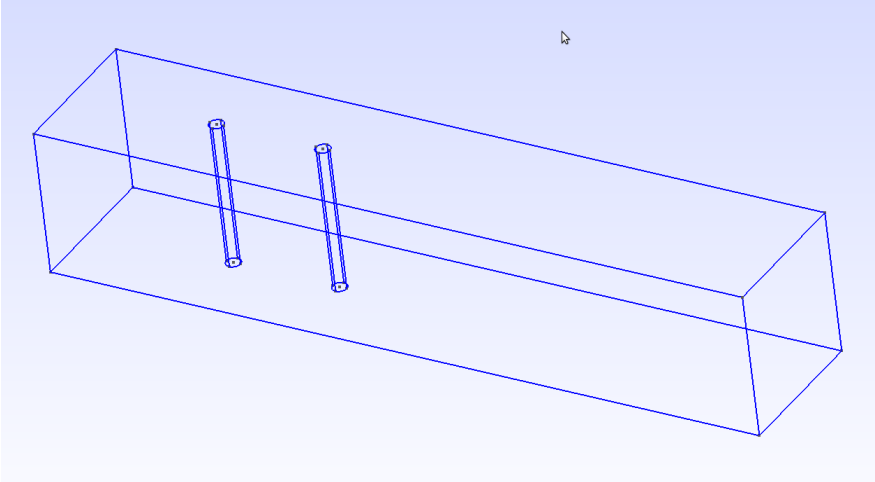

Figure 2: Geometry for the Depiction of Patches

corresponding to an air foil. This formula is shown below.

$$Re = \frac{V * c}{\nu} \tag{10}$$

The variable, c, corresponds to the chord length of the air foil. For this simulation, the chord length was equal to the diameter of the cylinder. Nu, is the kinematic viscosity of the fluid which is flowing. The kinematic viscosity used in this simulation was 0.0005 meters squared per second. Using all of these variables a Reynolds Number of 1600 was obtained. Additional parameters were needed as inputs for files corresponding to the specific RAS version of pisoFoam when using the k-epsilon model. Those parameters included the turbulence kinetic energy, turbulence dissipation rate, and turbulence intensity previously mentioned in the Mathematical Modeling section of the report. For our model, we calculated values of $k = 0.389$, $\epsilon = 113.5$. Our simulation has a turbulent intensity of 0.0636.

Validation

Because of the physics pertaining to the problem, certain areas of the domain required more refining than others. Areas closest to the cylinder walls needed to be as refined as possible while the areas farther away and closest to the edge of the domain would not need to be as refined. This is due to the fact that we are only concerned with the effects of the fluid flow on the cylinders. Ideally, we would want to create a mesh with volumes of equal sizes everywhere in the domain; however, a varied mesh works well to save computing time by achieving computational simplicity. In OpenFOAM, we still have to develop a three-dimensional mesh for our two-dimensional problem. In order to satisfy this condition, the mesh was generated in the x- and y- plane while a constant depth of one volume was set for the z-plane.

For this project, instead of using *blockMesh* we used *GeoMesh* to generate our mesh. This made refining our mesh a lot easier because now there are multiple cylinders in the domain instead of just one. In order to refine our mesh, we established a characteristic length for both the domain and the cylinders, named

$H_{farfield}$ and H_{circle}, respectively. H_{circle} was set to be smaller than $H_{farfield}$ in order to ensure that the volumes around the circle were smaller than those at the edge of the domain. So, as we move farther from the cylinders and closer to the edge of the domain, the characteristic length increases that of the cylinder, H_{circle}, to that of the domain $H_{farfield}$. Images of our starting mesh and final refined mesh are shown below. For our coarsest mesh, the values of $H_{farfield}$ and H_{circle} were both 0.1. However, in our final mesh the values of $H_{farfield}$ and H_{circle} were 0.025 and 0.005, respectively.

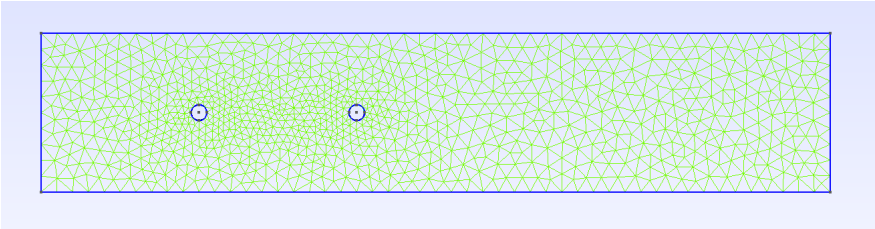

Figure 3: Coarsest Mesh: 1926 cells

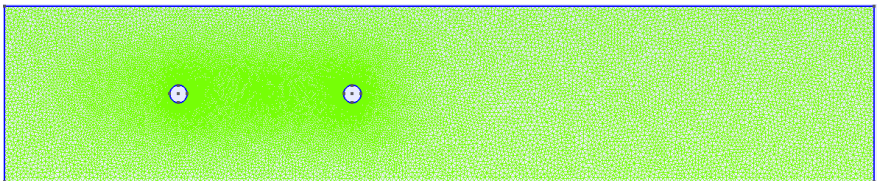

Figure 4: Final Mesh: 40,454 cell

One interesting thing to mention is our adjustment of the time step. Although our simulation was not time-dependent because our input velocity is considered to be constant, it was necessary for us to adjust our time step in OpenFOAM to make sure that the simulation did indeed run with these new turbulent properties. We believe that this small time step was needed to give the solver more time to record the various movements happening with the turbulent flow in the domain. Our time step decreased drastically from our midterm value of 0.025 to a value of $3.125e-04$.

Results

As stated previously, the purpose of our analyses was to minimize the collective drag forces over two cylinders. Below is a table of the forces recorded on the two cylinders, along with their distances from each other.

In addition to the above forces, some of the velocity and pressure profiles from our simulations are shown below. Figures 5 and 6 will show the respective profiles when the moving cylinder was 0.1 meters to the left of the stationary cylinder. Figures 7 and 8 will show the profiles when the moving cylinder was 0.2 meters to the right of the stationary cylinder. Figures taken at these placements of the moving cylinder were chosen because they were where the lowest drag forces were recorded on each side of the cylinder. Figures 9 and 10 will depict the profiles from when the moving cylinder was to the left of and adjacent to the stationary cylinder when A equaled 0.9. These profiles were chosen to be displayed because while the corresponding

Table 3: Average Forces on Both Cylinders

Distance (m)	**A**	**Forces (N)**
Left 0.3	0.6	2.94568
Left 0.15	0.75	1.68638
Left 0.1	0.8	−0.02421087
Left 0.05	0.85	0.145058
0	0.9	0.0663034
0	1.1	3.43483
0.025	1.125	2.97048
0.05	1.15	3.12796
0.075	1.175	3.39296
0.1	1.2	2.99873
0.15	1.25	3.27752
0.2	1.3	2.8839
0.25	1.35	3.43483
0.4	1.5	3.30783
0.9	2	3.58509
1.15	2.25	3.51291
1.4	2.5	3.51399
1.65	2.75	3.50574
1.9	3	3.51466
2.15	3.25	3.51458
2.4	3.5	3.51413
2.65	3.75	3.4909
2.9	4	3.46791

position for them is not where the net lowest drag force on the cylinders it is where the net lowest postive drag force was recorded.

Figure 5: Velocity Profile for Cylinder Placement 0.1 meter to the left for A = 0.8

Figure 6: Pressure Profile for Cylinder Placement 0.1 meter to the left for A = 0.8

Figure 7: Velocity Profile for Cylinder Placement 0.2 meter to the right for A = 1.3

Discussion

From all the simulations we ran, as can be shown within Table 3 of the Results section, the lowest net drag force recorded was when the moving cylinder was placed 0.1 meters to the left of the stationary cylinder during the simulation when A equaled 0.8. The data recorded from when the moving cylinder was placed to

Figure 8: Pressure Profile for Cylinder Placement 0.2 meter to the right for A = 1.3

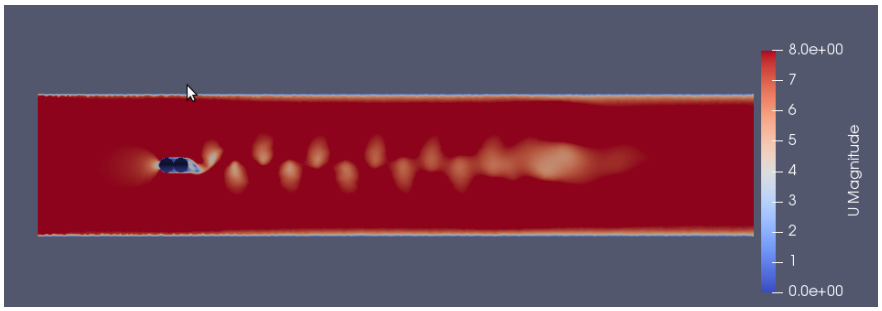

Figure 9: Velocity Profile for Cylinder Placement left and adjacent when A = 0.9

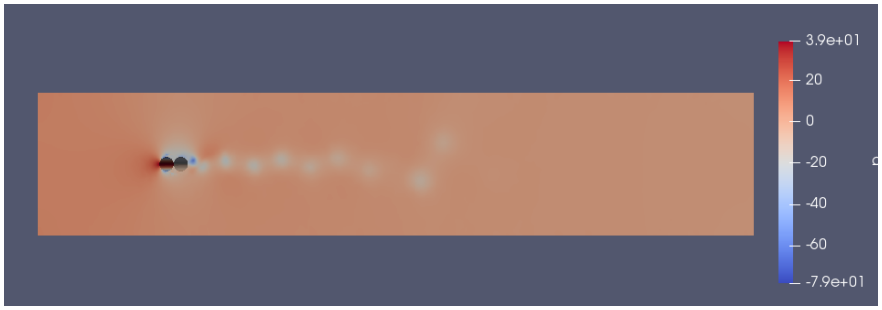

Figure 10: Pressure Profile for Cylinder Placement left and adjacent when A = 0.9

the left of the stationary cylinder supports an overall trend of drag reduction with a decrease in the distance between cylinders.

However, there were some very interesting occurrences. When the moving cylinder was moved from 0.1 to 0.05 meters to the left of the stationary cylinder there was a slight increase in drag. Also, when the same cylinder was placed to the right of the cylinder, the data fluctuated more than expected. However, not dissimilar to the data when the cylinder was placed to the left of the stationary cylinder, the positions for which the moving cylinder was closest to the stationary one tended to have the lowest collective drag forces overall. In fact, the lowest recorded amount of drag force measured from the placement of the moving cylinder to the right of the stationary occurred when they were only 0.2 meters apart. In addition to this, past a distance of 0.9 meters between the two cylinders, when the moving cylinder was placed to the right of the stationary one the drag force seemed to reduce without too much fluctuation.

Some of this phenomena may be explained by what was observed when viewing the velocity and pressure profiles in ParaView. Over the many simulations ran, the velocity profiles stayed fairly constant only having greater fluctuations when the cylinders were placed the closest together from either the left or the right. Because the velocity controls the skin friction drag, this suggests that there was little change in this factor going towards the total drag for most simulations. On the other hand, the pressure drag fluctuated a lot more. Based on this, it may be inferred that because skin friction and pressure drag are the two maintain components of drag from a fluid, those positions of the moving cylinder that best reduced the pressure drag had the lowest total drag forces. This suggests that for the moving cylinder positions both at 0.1 meters to the left and 0.2 meters to the right apart from the stationary cylinder the conditions were conducive to doing this. Both profiles also showed just a general reduction in change of both velocity and pressure profiles past about 0.9 meters apart to the right of the stationary cylinder. This corresponds with the general decrease in net drag with increasing distance between the cylinders past that point.

Other phenomena may be explained via comment made both by yourself and another student in class. Originally, the option to omit the data from the values of drag when the moving cylinder was placed to the left of the stationary one was considered due to that being desired. This desire was due to a theory that the second cylinder while to the left of the stationary one was too close to the inlet to pick up the full extent of the flow and it probably is. However, the fact is that at those distances the drag forces were some of the lowest collective drag forces recorded with the exact lowest being at 0.1 meters to the left of the stationary cylinder. The whole purpose of the simulations was to reduce drag, so in a round-about way that data is relevant.

Conclusions

The goal of this project was to reduce the drag between two cylinders and we believe that we have achieved the goal with regards to the situation with the parameters that were chosen. While it may have originally seemed like there should be one optimal distance for which the drag is reduced, understanding of the conditions conducive to reducing drag via the results of our simulations prove otherwise.

Based on those results, how drag is reduced depends on the flexibility of placement of the cylinders with respect to the inlet of the flow. Should the cylinders not be constrained by any additional parameters that were not addressed in our simulations, then putting the second cylinder closer to the inlet should reduce drag just as it did in our simulations by not letting the flow gain momentum. However, should a constraint exist and the moving cylinder is not able to be placed at the optimal distance of 0.1 meters to the left of the stationary cylinder, then it should be placed approximately 0.2 meters to the cylinder's right assuming the stationary cylinder is centered one meter from the outlet.

Additional simulations should be done in the future with the stationary cylinder as close as possible to the inlet so that the factor of just moving the second cylinder behind it can be isolated to determine the optimum distance apart in a single direction the cylinders should be. Also, additional cylinders to the original two should be modeled and orientations should be modified to see if there is an optimum set-up for which drag would be reduced since we only considered movement in a single direction. Furthermore, our research and simulations proved the successful reduction of drag between two cylinders.

References

[1] Md.Mahbub Alam, M Moriya, K Takai, and H Sakamoto. Fluctuating fluid forces acting on two circular cylinders in a tandem arrangement at a subcritical Reynolds number. *Journal of Wind Engineering and Industrial Aerodynamics*, 91(1-2):139–154, jan 2003.

[2] B.S. Carmo and J.R. Meneghini. Numerical investigation of the flow around two circular cylinders in tandem. *Journal of Fluids and Structures*, 22(6-7):979–988, aug 2006.

[3] H. Sakamoto and H. Haniu. Aerodynamic forces acting on two square prisms placed vertically in a turbulent boundary layer. *Journal of Wind Engineering and Industrial Aerodynamics*, 31(1):41–66, oct 1988.

[4] S.J. Price and M.P. Paidoussis. The aerodynamic forces acting on groups of two and three circular cylinders when subject to a cross-flow. *Journal of Wind Engineering and Industrial Aerodynamics*, 17(3):329–347, sep 1984.

[5] D. Sumner. Two circular cylinders in cross-flow: A review. *Journal of Fluids and Structures*, 26(6):849–899, aug 2010.

[6] OpenFOAM: applications/solvers/incompressible/pisoFoam/pisoFoam.C File Reference. https://www.openfoam.com/documentation/cpp-guide/html/pisoFoam$_8C.html details. Accessed on Tue, December 11, 2018.

[7] OpenFOAM: k-epsilon. https://www.openfoam.com/documentation/cpp-guide/html/guide-turbulence-ras-k-epsilon.html. Accessed on Tue, December 11, 2018.